Optical Clock Recovery and 3R Regeneration for 10-Gb/s NRZ Signal to Achieve 10 000-hop Cascadability and 1 000 000-km Transmission

Masaki Funabashi, Zuqing Zhu, Zhong Pan, Loukas Paraschis, and S. J. B. Yoo, *Senior Member, IEEE*

***Abstract*—This letter experimentally demonstrates all-optical clock recovery and optical 3R regeneration for a 10-Gb/s nonreturn-to-zero (NRZ) format. The 3R regenerator has achieved 10 000-hop cascadability and 1 000 000-km transmission for a pseudorandom bit sequence (PRBS) of $2^7 - 1$. A semiconductor-optical-amplifier-based Mach–Zehnder interferometer (SOA-MZI) as an NRZ to pseudoreturn-to-zero converter and a Fabry–Pérot filter perform the all-optical clock recovery from an NRZ signal. A pair of SOA-MZIs combined with a synchronous modulator provides the 2R regeneration and retiming functions. The cascadablity of the 3R regenerator is investigated in a recirculating loop transmission experiment by eye diagram, bit-error rate, and Q-factor measurements. Transmission with the 3R regenerator shows significant performance improvement over that without 3R regeneration. A 100-hop cascadability is also demonstrated for PRBS $2^{31} - 1$, enabling 10 000-km error-free transmission with a low power penalty of 1.2 dB.**

***Index Terms*—All-optical clock recovery, Fabry–Pérot filter (FPF), nonreturn-to-zero (NRZ) format, optical regeneration, semiconductor-optical-amplifier-based Mach–Zehnder interferometer (SOA-MZI).**

I. Introduction

ALL-OPTICAL signal regeneration is a key technology for future all-optical networking. "3R" regeneration, which performs the full functions of reamplification, reshaping, and retiming, is particularly attractive, because it can improve signal quality in both the amplitude and time domains. Although numerous publications have reported on various types of optical 3R regenerators, many of them employ a return-to-zero (RZ) data format [1], [2]. Compared to the RZ format, the nonreturn-to-zero (NRZ) format features a narrower spectral width suitable for dense wavelength-division multiplexing (WDM) and a higher tolerance to wavelength dispersion. Thus, the NRZ format is widely used in the current dense WDM and other systems. On the other hand, optical clock recovery from an NRZ signal is relatively challenging, because an NRZ signal has very weak clock components, especially for bit patterns supporting continuous "1"s and "0"s. While a number of previous publications reported on optical clock recovery from an NRZ signal [4]–[6], they did not incorporate it into a 3R regenerator. A few papers [7], [8] discuss optical 3R regeneration for the NRZ format, where electrical clock recovery was employed.

This letter demonstrates optical 3R regeneration for the NRZ data format as well as all-optical clock recovery from the NRZ signal. The proposed 3R regenerator utilizes semiconductor-optical-amplifier-based Mach–Zehnder interferometer (SOA-MZI) wavelength converters in both the clock recovery and the 3R regeneration processes. The cascadability of the 3R regenerator is investigated through recirculating loop transmission experiments. Transmission with 3R regeneration shows improved performance over that without 3R regeneration.

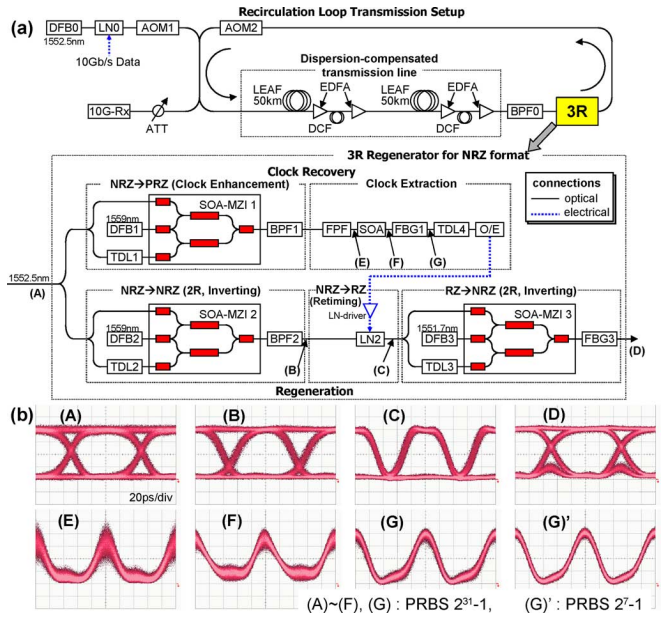

Fig. 1. (a) Experimental setup for 3R regeneration of an NRZ signal and for recirculating loop transmission. (b) Eye diagrams at the monitor locations (A)–(G) in the setup.

II. Experimental Setup

Fig. 1(a) and (b) shows the experimental setup and eye diagrams measured at the monitor locations (A)–(G) in the setup. The experiments utilize a recirculating loop transmission setup to evaluate the cascadability of a 3R regenerator at an inline location. The 100-km dispersion-compensated transmission line consists of two sets of 50-km LEAF fibers followed by a two-stage erbium-doped fiber amplifier and a dispersion-compensating fiber (DCF). The input power levels to the LEAF and

Manuscript received May 3, 2006; revised July 21, 2006. This work was supported in part by Furukawa Electric, Cisco System URP Program, and by the National Science Foundation under NSF 0335301 and NSF 9986665.

M. Funabashi is with the Department of Electrical and Computer Engineering, University of California, Davis, CA 95616 USA, and also with The Furukawa Electric Co., Ltd., Yokohama 220-0073, Japan.

Z. Zhu, Z. Pan, and S. J. B. Yoo are with the Department of Electrical and Computer Engineering, University of California, Davis, CA 95616 USA (e-mail: yoo@ece.ucdavis.edu).

L. Paraschis is with Advanced Technology, Core Routing, Cisco Systems, San Jose, CA 95134 USA.

Color versions of Figs. 1–5 are available online at http://ieeexplore.ieee.org.

Digital Object Identifier 10.1109/LPT.2006.883247

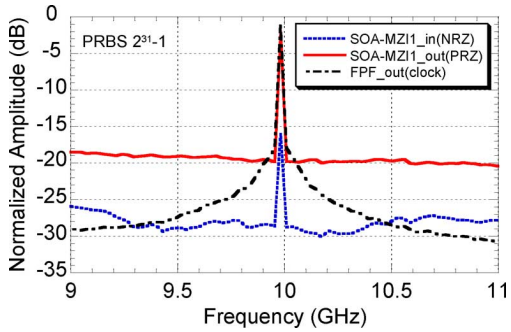

Fig. 2. RF spectra before and after NRZ-to-PRZ conversion and after FPF.

DCF fibers are 5 and −3 dBm, respectively. The measured optical signal-to-noise ratio and the estimated residual dispersion at the 3R regeneration input are 37.7 dB (0.1-nm bandwidth) and 22 ps/nm, respectively.

The operation principle of the 3R setup is described in [9]. The SOA-MZI1 converts the incoming NRZ signal into a pseudoreturn-to-zero (PRZ) signal and amplifies the weak 10-GHz clock component. Fig. 2 compares the two RF spectrum traces ("NRZ" and "PRZ"). The subsequent Fabry–Pérot filter (FPF) suppresses the broad spectral components attributed to the NRZ data modulation and extracts the clock component [5], [10], as seen in the trace ("clock") of Fig. 2. However, the eye diagram (E) in Fig. 1(b) for the recovered optical clock signal at the FPF output contains strong pattern-dependent amplitude variations. Although the subsequent saturated SOA and the fiber Bragg grating filter (FBG1, 0.22-nm bandwidth) suppress the amplitude variations, these variations subtly appear in the eye diagrams (F) and (G) of Fig. 1(b) when pseudorandom bit sequence (PRBS) $2^{31}-1$ is used. The recovered optical clock becomes better defined with the short word length of PRBS $2^{7}-1$, as seen in (G). The optical-to-electrical converter [(O/E) Agilent 11982A] with a 15-GHz bandwidth converts the optical recovered clock signal into an electrical signal that synchronously modulates the data stream for retiming. Note that the O/E conversion can be avoided by substituting the recovered optical clock signal for the continuous-wave light (DFB2) [11].

The two wavelength converters (SOA-MZI2&3) operating in the inverting mode provide 2R regeneration while preserving the signal wavelength and polarity. Since the inverting mode SOA-MZIs offer a better noise clamping property on the mark level of their input signal, both of the mark and space levels are reshaped effectively through the pair of inverting-mode SOA-MZIs. The synchronous modulator LN2 driven by the recovered clock signal provides a retiming function, as well as NRZ-to-RZ conversion. The SOA-MZI3 converts the RZ format back to the NRZ format. The eye diagrams (B)–(D) show clear eye openings and high extinction ratios.

III. Experimental Results and Discussion

Fig. 3 shows the eye diagrams after the various recirculating loop transmission experiments. When the 3R regeneration block in Fig. 1(a) is removed, the eye diagrams in Fig. 3(a) (1R only) sustain good eye openings up to Lap10, but they begin to suffer from amplitude and timing jitter noise accumulations above Lap10. Next, the 3R regeneration block is introduced but the driver for the synchronous modulator is turned "OFF" to see transmission performance without retiming. The eye diagrams

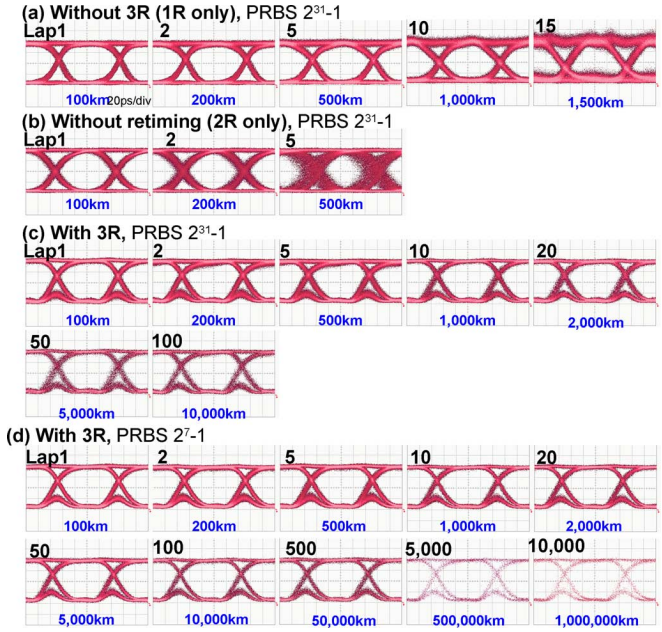

Fig. 3. Eye diagrams after recirculating loop transmission experiments (a) without 3R (1R only), (b) without retiming (2R only), (c) with 3R (PRBS $2^{31}-1$), and (d) with 3R (PRBS $2^{7}-1$). Numbers at the upper left and at the bottom are lap number and transmission distance, respectively.

in Fig. 3(b) (2R only) show the reshaped mark and space levels but exhibit severe timing jitter noise accumulation at a relatively small lap number. This severe timing jitter noise is induced by the pattern-dependent carrier distribution that takes places in the SOAs of the wavelength converters [12]. However, when full 3R function including retiming is implemented, almost identical eye diagrams are obtained from Lap1 to Lap100, as seen in Fig. 3(c). These results indicate that both of the reshaping and retiming functions work effectively, suppressing the amplitude and timing jitter noise accumulations observed in the "1R only" and "2R only" cases. To investigate the pattern length dependence, we also measured the eye diagrams in Fig. 3(d) for PRBS $2^{7}-1$, which show slightly better eye openings especially in the time domain, compared to those in Fig. 3(c) for PRBS $2^{31}-1$.

Fig. 4 shows BER curves after the recirculating loop transmission experiments for 1R only, 2R only, and 3R, which corresponds to the results of Fig. 3(a)–(c), respectively. For 1R only, the power penalty steadily increases with the lap number, and the power penalty from Lap1 to Lap10 is 1.2 dB at a BER of 1×10^{-9}. The Lap5 curve for 2R only shows bending and an error floor around $\sim 3\times10^{-8}$. With 3R regeneration, there is a power penalty of about 0.5 dB at Lap1 compared to the curve of 1R_Lap1. However, all of the BER curves show error-free operations below 1×10^{-10}, and the power penalties are less than 1.2 dB at 1×10^{-10} for up to Lap100, compared to the back-to-back result.

Fig. 5 depicts the measured Q-factor as a function of transmission distance. The upper horizontal axis shows the corresponding lap number. The Q-factors are measured from BER versus threshold voltage curves, with a constant optical input power of −15 dBm into the receiver (10G-Rx). In the cases of 1R and 2R, the Q-factors begin to decrease rapidly around Lap10 and Lap 3, respectively, which is consistent with the trend

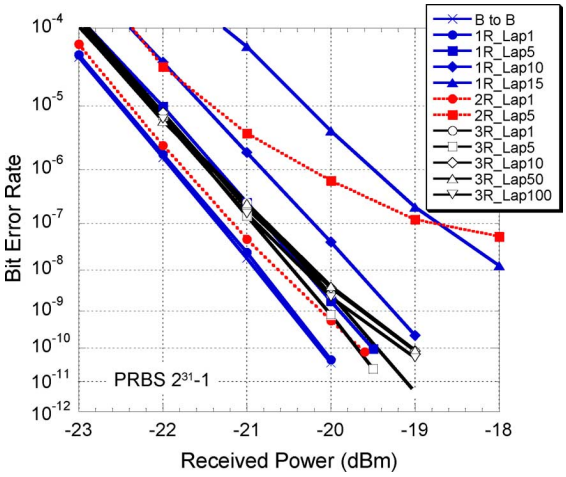

Fig. 4. BER curves after recirculating loop transmission experiments with 1R only, 2R only, and 3R regeneration.

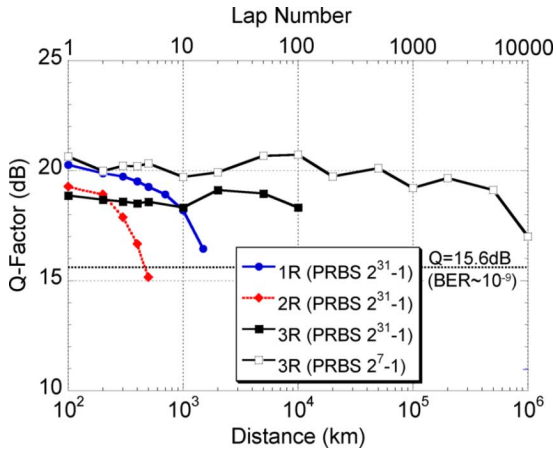

Fig. 5. Q-factor versus transmission distance and lap number for recirculating loop transmission with 1R only, 2R only, and 3R regeneration.

observed in the eye diagrams and the BER curves. With 3R regeneration, the two word lengths of PRBS 2^7-1 and $2^{31}-1$ are tested. The Q-factors for PRBS $2^{31}-1$ remain almost constant around 18 dB up to Lap100, which corresponds to a transmission distance of 10 000 km. The Q-factors for PRBS 2^7-1 remain slightly higher around 20 dB up to Lap100. The Q-factor at Lap10000 (1 000 000 km in distance) is still higher than 15.6 dB that corresponds to a BER level of 10^{-9}, although the Q-factors show gradual degradation beyond Lap100.

Compared to the results in [3], which demonstrated 10 000-hop cascaded 3R regeneration with a PRBS $2^{23}-1$ RZ signal, these results indicate that the FPF-based clock recovery from the NRZ signal via NRZ-to-PRZ conversion is more sensitive to word length than that from the RZ signal. We consider the reason for this difference to be as follows. First, even with the NRZ-to-PRZ conversion, there is an absence of output pulses during both long zeros ("0"s) and long ones ("1"s) in the incoming NRZ bit patterns. The pulse absence does not contribute to generating the recovered clock signal in the FPF, while long ones can contribute to the clock recovery in the case of RZ input. Second, the amplitude noise in the incoming NRZ signal can transfer onto the timing jitter noise in the PRZ signal during the NRZ-to-PRZ conversion. These factors result in the acceleration of the timing jitter accumulation, especially when the word length is long. The timing jitter caused by the first factor can be improved with the use of a higher finesse FPF or a high-Q RF filter after the O/E converter. Although the 3R setup in Fig. 1(a) splits the incoming signal in front of the SOA-MZI2 to feed it to the clock recovery circuit, splitting and feeding the signal at the SOA-MZI2 output after reshaping will mitigate the timing jitter caused by the second factor.

IV. Conclusion

We have proposed and demonstrated an NRZ format 3R regenerator in 10-Gb/s recirculating loop transmission experiments. An SOA-MZI-based NRZ-to-PRZ converter combined with an FPF performed clock recovery from the NRZ signal. A pair of SOA-MZI wavelength converters and a synchronous modulator provided the 3R regeneration function. The transmission system with the 3R regenerator improves the signal quality, cascadability, and transmission distance, compared to that without 3R regeneration. The 3R regenerator has achieved 100-hop cascaded error-free transmission (10 000 km in distance) with a 0.3-dB power penalty for the 10-Gb/s PRBS $2^{31}-1$ NRZ signal. Cascadability up to 10 000 hops, which corresponds to a transmission distance of 1 000 000 km, is also demonstrated with a shorter word length of PRBS 2^7-1. The optical 3R regeneration method discussed here can be applied to multichannel transmission systems. The possibility of realizing a compact multichannel all-optical regeneration module without concerns for electromagnetic interference in multichannel electronics also motivates further studies of this technology in the context of WDM transmission systems.

References

[1] G. Raybon *et al.*, "40 Gbit/s pseudo-linear transmission over one million kilometers," in *Proc. OFC 2002*, Anaheim, CA, Paper FD10.

[2] B. Lavigne, P. Guerber, P. Brindel, E. Balmefrezol, and B. Dagens, "Cascade of 100 optical 3R regenerators at 40 Gbit/s based on all-active Mach Zehnder interferometers," in *Proc. ECOC'01*, 2001, vol. 3, pp. 290–291.

[3] Z. Zhu, M. Funabashi, Z. Pan, L. Paraschis, and S. J. B. Yoo, "10 000-hop cascaded in-line all-optical 3R regeneration to achieve 1 250 000-km 10-Gb/s transmission," *IEEE Photon. Technol. Lett.*, vol. 18, no. 5, pp. 718–720, Mar. 1, 2006.

[4] C. Kim, I. Kim, X. Li, and G. Li, "All-optical clock recovery of NRZ data at 40 Gbit/s using Fabry–Perot filter and two-section gain-coupled DFB laser," *Electron. Lett.*, vol. 39, pp. 1456–1458, 2003.

[5] G. Contestabile, M. Presi, N. Calabretta, and E. Ciaramella, "All-optical clock recovery from 40 Gbit/s NRZ signal based on clock line enhancement and sharp periodic filtering," *Electron. Lett.*, vol. 40, pp. 1361–1362, 2004.

[6] J. Slovak, C. Bornholdt, J. Kreissl, S. Bauer, M. Biletzke, M. Schlak, and B. Sartorius, "Bit rate and wavelength transparent all-optical clock recovery scheme for NRZ-coded PRBS signals," *IEEE Photon. Technol. Lett.*, vol. 18, no. 7, pp. 844–846, Apr. 1, 2006.

[7] D. Chiaroni *et al.*, "New 10 Gbit/s 3R NRZ optical regenerative interface based on semiconductor optical amplifiers for all-optical networks," in *Proc. ECOC'97*, 1997, vol. 5, pp. 41–44.

[8] H. S. Chung, R. Inohara, K. Nishimura, and M. Usami, "40-Gb/s NRZ wavelength conversion with 3R regeneration using an EA modulator and SOA polarization-discriminating delay interferometer," *IEEE Photon. Technol. Lett.*, vol. 18, no. 2, pp. 337–339, Jan. 15, 2006.

[9] M. Funabashi *et al.*, "First field demonstrations of 1000-hop cascaded all-optical 3R regeneration in 10 Gb/s NRZ transmission," in *Proc. CLEO'06*, Long Beach, CA, 2006, Paper CPDB7.

[10] G. T. Kanellos *et al.*, "Clock and data recovery circuit for 10-Gb/s asynchronous optical packets," *IEEE Photon. Technol. Lett.*, vol. 15, no. 11, pp. 1666–1668, Nov. 2003.

[11] B. Lavigne *et al.*, "Test at 10 Gbit/s of an optical 3R regenerator using an integrated all-optical clock recovery," in *Proc. ECOC'99*, 1999, pp. 262–263, Paper Th A2.3.

[12] A. Kloch *et al.*, "Accumulation of jitter in cascaded wavelength converters based on semiconductor optical amplifiers," in *Proc. OFC'99*, 1999, vol. 4, pp. 33–35.